Molecular Biology of the Cell
Vol. 15, 2509–2522, May 2004

Genetic Dissection of Meiotic Cytokinesis in *Drosophila* Males[D]

Maria Grazia Giansanti,*† Rebecca M. Farkas,†‡ Silvia Bonaccorsi,* Dan L. Lindsley,§ Barbara T. Wakimoto,‖ Margaret T. Fuller,‡ and Maurizio Gatti*¶

*Istituto Pasteur Fondazione Cenci Bolognetti and Istituto di Biologia e Patologia Molecolari del CNR, Dipartimento di Genetica e Biologia Molecolare, Universitá "La Sapienza," Rome, 00185 Italy; ‡Department of Developmental Biology and Department of Genetics, Stanford University School of Medicine, Stanford, California 94305-5329; §Section of Cell and Developmental Biology, Division of Biological Sciences, University of California, San Diego, La Jolla, California 92093-0349; and ‖Department of Biology and Center for Developmental Biology, University of Washington, Seattle, Washington 98195-1800

Submitted August 18, 2003; Revised January 29, 2004; Accepted February 13, 2004
Monitoring Editor: Ted Salmon

We have used *Drosophila* male meiosis as a model system for genetic dissection of the cytokinesis mechanism. *Drosophila* mutants defective in meiotic cytokinesis can be easily identified by their multinucleate spermatids. Moreover, the large size of meiotic spindles allows characterization of mutant phenotypes with exquisite cytological resolution. We have screened a collection of 1955 homozygous mutant male sterile lines for those with multinucleate spermatids, and thereby identified mutations in 19 genes required for cytokinesis. These include 16 novel loci and three genes, *diaphanous*, *four wheel drive*, and *pebble*, already known to be involved in *Drosophila* cytokinesis. To define the primary defects leading to failure of cytokinesis, we analyzed meiotic divisions in male mutants for each of these 19 genes. Examination of preparations stained for tubulin, anillin, KLP3A, and F-actin revealed discrete defects in the components of the cytokinetic apparatus, suggesting that these genes act at four major points in a stepwise pathway for cytokinesis. Our results also indicated that the central spindle and the contractile ring are interdependent structures that interact throughout cytokinesis. Moreover, our genetic and cytological analyses provide further evidence for a cell type-specific control of *Drosophila* cytokinesis, suggesting that several genes required for meiotic cytokinesis in males are not required for mitotic cytokinesis.

INTRODUCTION

Cytokinesis is the complex process that separates the daughter cells at the end of cell division. In animal cells, cytokinesis is mediated by an actomyosin ring that forms during late anaphase. This ring assembles just beneath the equatorial cortex and constricts while remaining anchored to the plasma membrane, thus mediating furrow ingression. At the end of cytokinesis, the actomyosin ring disassembles and addition of new membrane seals the remaining intracellular bridge, leading to the final separation (abscission) of the daughter cells (reviewed by Glotzer, 2001).

Although the main events and structures that mediate cytokinesis are well described, the molecular mechanisms underlying the process are still largely unknown. Genetic and biochemical analyses have allowed identification of only a few components of the contractile ring and proteins that regulate its assembly and disassembly. Structural components of the *Drosophila* contractile ring include actin, myosin II, the regulatory light chain of myosin II encoded by the *spaghetti squash* (*sqh*) gene (Karess at al., 1991), and anillin (Field and Alberts, 1995). Formation of the *Drosophila* cytokinetic ring is regulated by Rho, its upstream activator Rho GEF encoded by the *pebble* (*pbl*) gene (reviewed by Prokopenko *et al*., 2000), its downstream effector Diaphanous (Dia), and the Dia-interacting protein profilin encoded by the *chickadee* (*chic*) gene (reviewed by Wasserman, 1998). Actin ring disassembly is mediated by cofilin encoded by the *twinstar* (*tsr*) gene, consistent with actin filament severing activity of cofilins (Gunsalus *et al*., 1995).

Assembly of the F-actin ring seems to be intimately connected to the spindle. During late anaphase and telophase, the spindle of animal cells reorganizes to form the stembody, a dense network of antiparallel microtubules with their plus ends interdigitating at the center of the cell and their minus ends terminating not at the centrosomes but near the separating sets of chromosomes (Mastronarde *et al*., 1993). Here, we refer to this bundle of microtubules as "central spindle" and to its middle part as "central spindle midzone." In all animal systems analyzed to date, the integrity of the central spindle is essential for cytokinesis (reviewed by Gatti *et al*., 2000; Glotzer, 2001). Moreover, studies in *Drosophila* suggest that the central spindle and the contractile ring are interdependent structures (Giansanti *et al*.,

Article published online ahead of print. Mol. Biol. Cell 10.1091/mbc.E03–08–0603. Article and publication date are available at www.molbiolcell.org/cgi/doi/10.1091/mbc.E03–08–0603.

[D] Online version of this article contains supporting material. Online version is available at www.molbiolcell.org.

† These authors contributed equally to this work.

¶ Corresponding author. E-mail address: maurizio.gatti@uniroma1.it.

Supplemental Material can be found at:
http://www.molbiolcell.org/content/suppl/2004/03/05/E03-08-0603.DC1

1998; Somma *et al*., 2002). Mutations in proteins that are enriched at the central spindle midzone, such as the Klp3A and Pavarotti (Pav) kinesins, the Polo kinase that phosphorylates and coimmunoprecipitates Pav, and the Rho GTPase activating protein RacGAP50, which also forms a complex with Pav, disrupt both central spindle formation and contractile ring assembly (Williams *et al*., 1995; Adams *et al*., 1998; Carmena *et al*., 1998; Giansanti *et al*., 1998; Somma *et al*., 2002; Somers and Saint, 2003). Likewise, mutations in *rho1*, *pbl*, *sqh*, *dia*, and *chic*, which all encode proteins involved in actomyosin ring formation and function, also disrupt the assembly of both structures (Prokopenko *et al*., 1999; Giansanti *et al*., 1998; Somma *et al*., 2002). Together, these results suggest cooperative interactions between central spindle microtubules and elements of the actomyosin ring. However, the molecular mechanisms underlying these interactions remain poorly understood.

Further investigation is also needed to understand the role and mechanism of membrane formation during cytokinesis. Formation of new cortical membrane is thought to arise from the fusion of Golgi-derived vesicles that are targeted to the furrow through a microtubule-dependent transport mediated by kinesin-like proteins (Straight and Field, 2000; Skop *et al*., 2001). Consistent with a requirement for membrane addition to the cleavage furrow, *Drosophila*, *Caenorhabditis elegans*, and *Arabidopsis thaliana* syntaxins (Lauber *et al*., 1997; Jantsch-Plunger and Glotzer, 1999; Somma *et al*., 2002; Xu *et al*., 2002), a *Drosophila* phosphatidylinositol 4-kinase (Fwd; Brill *et al*., 2000), and the *Drosophila* Golgi associated Cog-5 protein (Fws; Farkas *et al*., 2003) have been shown to be required for cytokinesis. However, the complete pathway for membrane addition needs to be elucidated, and it is not known how membrane addition is coordinated with actomyosin ring constriction to drive cleavage furrow ingression.

As a fundamental step toward elucidating the molecular mechanisms of cytokinesis, we have undertaken a large-scale screen to identify new genes required for meiotic cytokinesis in *Drosophila* males. *Drosophila* male meiosis offers a highly suitable model system for the identification of cytokinesis mutants, due to the peculiar structure of *Drosophila* spermatids. Both premeiotic and meiotic divisions occur within a cyst; 16 primary spermatocytes undergo the first meiotic division synchronously, giving rise to 32 secondary spermatocytes, which in turn divide, producing 64 spermatids. During both meiotic divisions, mitochondria line up along the central spindle and partition equally between the two daughter cells. At the end of meiosis, the mitochondria inherited by each spermatid fuse to form a complex interlaced structure called the nebenkern. By the so-called onion stage, each wild-type spermatid contains a single round nucleus associated with a nebenkern of similar shape and size (Figure 1A). Mutations that cause defects in cytokinesis but not in karyokinesis disrupt proper mitochondria partitioning, resulting in spermatids with an abnormally large nebenkern associated with two or four normal-sized nuclei (Figure 1B; Fuller, 1993). *Drosophila* male meiosis is also highly suitable for a detailed cytological analysis of cytokinesis mutants. Due to the relatively large size of mature primary spermatocytes, meiotic spindles are large and display prominent central spindles (Cenci *et al*., 1994). These cells also exhibit striking actin-based contractile rings that assemble around the central spindle midzone during late anaphase and constrict throughout telophase (Gunsalus *et al*., 1995; Hime *et al*., 1996; Giansanti *et al*., 1998). In both gonial and meiotic divisions, cytokinesis is incomplete and daughter cells remain connected by cytoplasmic bridges called ring canals, which develop from arrested contractile rings and contain components of the cytokinetic apparatus such as anillin (Hime *et al*., 1996; Giansanti *et al*., 1999). Failures in cytokinesis often result in ring canals that are either larger or smaller than their wild-type counterparts, providing a further criterion for characterization of cytokinesis mutants (Hime *et al*., 1996; Giansanti *et al*., 1999).

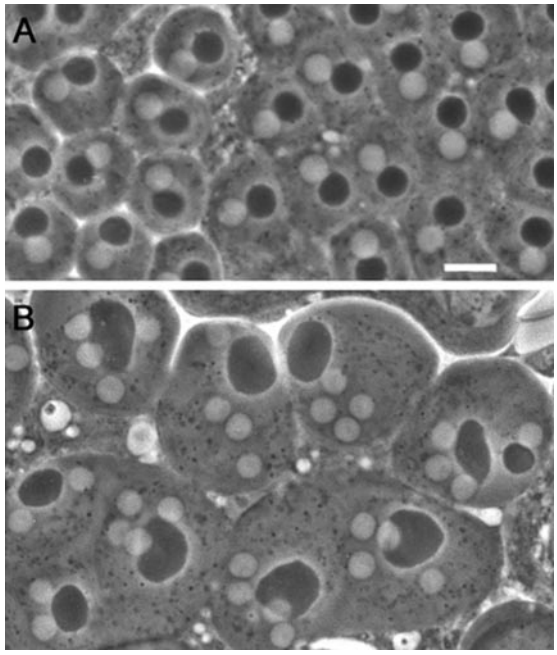

Figure 1. Spermatid morphology in wild-type males and in cytokinesis-defective mutants. Spermatids are viewed by phase contrast microscopy. (A) Wild-type spermatids containing a single phase-light nucleus associated with a single phase-dark nebenkern of similar size. (B) Spermatids from *funnel cakes* (*fun*) mutants containing a large nebenkern associated with four or two nuclei of regular sizes. Bar, 10 μm.

Here, we describe the isolation and characterization of mutants that define 16 novel genes required for spermatocyte cytokinesis. Our phenotypic analyses indicate that spermatocyte cytokinesis can be subdivided into discrete steps, and reveal interactions between different components of the cytokinetic machinery.

MATERIALS AND METHODS

Fly Strains and Mapping Experiments

From a collection of >12,000 lines maintained in the laboratory of Charles Zuker that carry, in balanced condition, either a second or a third chromosome that was treated with a heavy dose of ethyl methonesulfonate and shown to survive in homozygous condition (Koundajkian, Cowan, Hardy, and Becker, unpublished data), we isolated 1955 male-sterile mutations (Wakimoto, Lindsley, and Herrera, unpublished data). To identify mutants defective in spermatocyte cytokinesis, we screened mutant males from these 1955 lines for onion-stage spermatid morphology. The second chromosome lines, designated *Z0001* through *Z6079* for allele designations, carry a mutagenized second chromosome marked with *cn* and *bw* balanced over *CyO*, *Cy cn*^{2}. The third chromosome lines, designated *Z0001* through *Z6257* for allele designations, are homozygous for *bw* and carry a *st*-marked mutagenized third chromosome over the *TM6B*, *Hu e Tb* balancer. Complementation tests were performed between all appropriate pairs of mutations, and with the *chic*^{R1}, *dia*^{1}, *tsr*^{ms2651}, *fwd*^{3}, *pbl*^{5}, *pav*^{B200}, *polo*^{1}, and *polo*^{1673} mutant alleles (FlyBase; http://morgan.harvard.edu/). Mutations on chromosome 2 were mapped by recombination by the use of multiply marked chromosomes with *al dp b pr c px sp* and *al dp b pr Bl c px sp*, and tested for failure to complement the deletions from the chromosome 2 deficiency kit provided by the Bloom-

ington Stock Center (Department of Biology, Indiana University, Bloomington, IN). Mutations on chromosome 3 were mapped by recombination using the *rucuca* and *ruPrica* multiply marked chromosomes and tested for failure to complement the chromosome 3 deficiency kit from Bloomington Stock Center. Visible markers, balancer chromosomes, and deficiencies are described in detail by Lindsley and Zimm (1992) and in FlyBase (http://morgan.harvard-.edu/).

Flies were raised on standard *Drosophila* medium. Complementation tests and mapping experiments were performed at 25°C.

In Vivo Analyses

To define the spermatid phenotype of cytokinesis-defective mutants, late larval or early pupal testes were examined in living squashed preparations by phase contrast microscopy, as described by Regan and Fuller (1990). To view live spermatocytes undergoing cytokinesis, larval or pupal testes were dissected under Voltalef 20S oil, as described by Brill *et al.* (2000). Images were recorded at 1-min intervals using a charge-coupled device camera (Photometrics, Tucson, AZ) and the IP Lab software. The Oregon R stock was used as a wild-type control for all in vivo phenotypic analyses.

Fixation and Staining Procedures

Testis dissection, fixation, and staining were performed at room temperature. Cytological preparations were made with testes from third instars or young pupae. For simultaneous visualization of either tubulin and actin, or anillin and actin, testes were dissected and fixed according to Gunsalus *et al.* (1995). Anillin immunostaining and actin staining were then carried out as described by Giansanti *et al.* (1999). The anti-anillin antibody was raised against amino acids 1 through 371 (Field and Alberts, 1995). For simultaneous visualization of tubulin and anillin, testes were dissected and fixed according to Cenci *et al.* (1994) and then stained as described by Giansanti *et al.* (1999). Double immunostaining of KLP3A and tubulin was carried out as described by Williams *et al.* (1995). In all cases, slides were mounted in Vectashield with 4,6 diamidino-2-phenylindole (Vector Laboratories, Burlingame, CA) to stain DNA and reduce fluorescence fading.

Immunostained preparations were examined with an Axioplan fluorescence microscope (Carl Zeiss, Oberkochen, Germany), equipped with an HBO 50-W mercury lamp and a cooled charged-coupled device camera (Photometrics), as described previously (Giansanti *et al.*, 1999). Gray scale digital images were collected separately using the IP lab Spectrum software and converted to Photoshop format.

RESULTS

Isolation of Cytokinesis Mutants

To isolate mutations affecting cytokinesis during *Drosophila* male meiosis, we screened a collection of 1955 lines carrying ethyl methonesulfonate-induced mutations that cause male sterility. These sterile lines were isolated from ~12,000 viable lines, generated in C. Zuker's laboratory (see MATERIALS AND METHODS). Analysis by phase-contrast microscopy revealed that 64 of these male sterile lines produced spermatids with an abnormally large nebenkern and multiple normal-sized nuclei, indicating defects in cytokinesis but not in chromosome segregation. Twenty-six of these 64 lines showed <20% abnormal spermatids, most of which had a large nebenkern associated with only two nuclei. Although potentially interesting, these mutant lines were not studied further because their meiotic abnormalities were too rare to allow cytological analysis of the cytokinetic defect (see below).

We next performed inter se complementation tests among the remaining 11 second chromosome lines and the remaining 27 third chromosome mutant lines. The analysis of spermatid morphology in each heteroallelic combination led to identification of 23 complementation groups, seven on the second and 16 on the third chromosome. Representative mutant alleles from these groups were then tested for complementation with several known *Drosophila* cytokinesis mutations. Mutations in one of the complementation groups on chromosome 2 were allelic to *diaphanous* (Castrillon and Wasserman, 1994). Two of the complementation groups on chromosome 3 proved to be *pebble* (Hime and Saint, 1992; Lehner, 1992) and *four wheel drive* (Brill *et al.*, 2000). No new alleles of *chickadee* (Cooley *et al.*, 1992), *pavarotti* (Adams *et al.*, 1998), *polo* (Sunkel and Glover, 1988), or *twinstar* (Gunsalus *et al.*, 1995) were identified.

Representative strong alleles of the remaining 20 complementation groups were mapped by meiotic recombination and tested for failure to complement a set of deficiencies that, together, deleted more than two-thirds of the appropriate chromosome. Both the recombination and deficiency mapping experiments were scored on the basis of the spermatid phenotype. In four of the third chromosome lines, the lesions responsible for the cytokinesis phenotype did not map to a single locus in recombination analysis, suggesting additive or synergistic effects of more than one mutation. In each case, the line was the only representative of its complementation group and was not studied further. For the remaining 16 complementation groups, the representative mutant allele analyzed behaved simply in recombination mapping and could be mapped to a single interval. In some cases, the interval could be narrowed down to a discrete chromosomal region defined by a deficiency that failed to complement the mutation for the spermatid phenotype (Table 1).

Each of the 19 complementation groups identified in our screen (the 16 new genes, *dia*, *fwd*, and *pbl*) contained mutant alleles that displayed high frequencies of abnormal spermatids (Table 2). Mutant males commonly had spermatids with a large nebenkern and two or four normal-sized nuclei (Figure 1B and Table 2), indicating failure of cytokinesis during one or both the meiotic divisions, respectively. Occasionally, spermatids with three nuclei were observed, suggesting failure of cytokinesis during the first meiotic division, followed by budding off of only one daughter cell during the second meiotic division (Table 2). A few mutants produced spermatids with eight or more nuclei, most likely due to defects in the mitotic divisions preceding meiosis (Table 2).

Cytological Characterization of Cytokinesis Mutants

To define the primary defects in cytokinesis leading to the formation of spermatids with multiple nuclei, we examined meiotic division in representative mutant males for each of the 19 genes identified in our screen. Testis preparations were stained with anti-tubulin antibodies to visualize spindle microtubules and with rhodamine-phalloidin to visualize the F-actin–based contractile ring. Testis preparations of all mutants were also immunostained for two additional proteins involved in *Drosophila* cytokinesis: anillin and Klp3A. Anillin is an actin-binding protein that accumulates at the equatorial cortex of ana-telophase cells (Field and Alberts, 1995; Hime *et al.*, 1996; Giansanti *et al.*, 1999), and Klp3A is a kinesin-like protein that concentrates at the central spindle midzone (Williams *et al.*, 1995).

In wild-type spermatocytes, anillin accumulates at the cell cortex during late anaphase, forming a circumferential band at the cell equator (Figure 2A). At this time, the central spindle has just begun to assemble and contains many antiparallel microtubules that overlap at the center of the cell (Figure 2A); the appearance of the anillin ring coincides with the first detectable accumulation of Klp3A at the spindle midzone (Giansanti *et al.*, 1999; Giansanti, Bonaccorsi and Gatti, unpublished observations). The F-actin contractile ring forms in a subsequent stage of ana-telophase and precisely colocalizes with the anillin band. Anillin and F-actin continue to colocalize throughout ring constriction, whereas the central spindle midzone continues to accumulate Klp3A and becomes increasingly pinched (Figures 2, 3, and 4). At the end of cytokinesis, the F-actin ring disassembles, whereas anillin becomes incorporated into a stable ring canal (Hime *et al.*, 1996; Giansanti *et al.*, 1999).

Table 1. Map positions of genes identified by cytokinesis-defective mutants

Locus	No. of alleles	Uncovering deficiency	Cytological position[a]	Map position[b]
bird nest soup (bns)	1	Not found		2–7.5 ± 3.1 (*al, dp*)
james bond (bond)	7	*Df(3R)hh*	93F11–94D13	3–75.5 ± 3.1 (*e, Pr*)
brunelleschi (bru)	2	*Df(2L)pr2b*	38B5-E1	2-(*b, c*)
celibe (cbe)	1	Not found		2–106.5 ± 0.7 (*px, sp*)
ciambella (cia)	2	Not found		2-(distal to *sp*)
diaphanous (dia)	2	*Df(2L)TW84*	38A1–39E1	2-(*b, c*)
fermata (fer)	2	Not found		3–75.5 (*sr, ca*)
four score (fsco)	2	*Df(3R)p25*	85A3–85B1	3-(*th, sr*)
four wheel drive (fwd)	2	*Df(3L)7C*	61B1–C1	3-(distal to *ru*)
four way stop (fws)	2	*Df(2L)qua*^{1374}	36C	2-(*b, pr*)
frodo (fro)	2	*Df(3L)AC1*	67A2–D13	3-(*th, cu*)
funnel cakes (fun)	1	Not found		3–48.8 ± 1.1 (*th, cu*)
giotto (gio)	1	*Df(3R)Dl-Bx12*	91F1–92D6	3-(*cu, ca*)
omelette (omt)	1	*Df(3R)e-F1*	93C6–E1	3-(*sr, ca*)
onion rings (onr)	1	*Df(3R)Espl1*	96F7–97A4	3–90.1 ± 0.9 (*Pr, ca*)
pebble (pbl)	1	*Df(3R)pbl-NR*	66B1–2	3-(*ru, h*)
sauron (sau)	1	Not found		2–7.1 ± 2.8 (*al, dp*)
scapolo (scpo)	1	Not found		3–59.1 ± 2.4 (*cu, sr*)
smeagol (sgo)	2	*Df(3R)mbc-R1*	95A5–D11	3–85.7 (*e, ca*)

[a] Published deficiency breakpoints.

[b] Determined by recombination. Flanking markers used for mapping are in parentheses.

Progression through telophase I involves morphological transformations of the spindle poles as well as of the central spindle and contractile ring. In early and mid-telophase I, each spindle pole displays a single centrosome that nucleates an astral array of microtubules. As telophase I progresses, the centrioles comprising each centrosome separate, giving rise to two separate asters that rotate toward the opposite sides of the nucleus, in preparation for the second meiotic division (Figures 2C and 3C). The contractile ring and the central spindle are usually nearly fully constricted by the time the asters looked separated (Figures 2C and 3C). Thus, aster separation provides a useful marker for identification of late telophase cells. We have used this marker to characterize the mutant phenotypes of primary spermatocytes undergoing the first meiotic division. However, we also examined the second meiotic division in all mutants. In all cases, the defects observed in telophase II cells were fully consistent with those seen in telophase I figures (our unpublished data).

An examination of preparations from mutant testes revealed that in one mutant, *fermata* (*fer*), most spermatocytes were very large and contained multiple dividing nuclei, consistent with the *fer* spermatid phenotype (Table 2). The presence of multiple, overlapping meiotic spindles within the same large cells (our unpublished data) precluded a reliable definition of the cytokinesis defect of this mutant. The other 18 mutants, however, displayed discrete defects in components of the cytokinetic machinery (Table 3). Based on our phenotypic analyses, we divided the genes identified by these mutations into the four classes described below.

Genes Required for Anillin Localization, Central Spindle Formation, and Contractile Ring Assembly

Double staining of *pbl* spermatocytes for either anillin and tubulin or F-actin and tubulin revealed that wild-type function of *pbl* is required for the assembly of all the major structures present at the equator of spermatocytes in ana-telophase. Spermatocytes from *pbl* homozygotes or hemizygotes lacked the anillin cortical band throughout anaphase and telophase (n = 150; Figure 5, A and B). In addition, ana-telophase spermatocytes from *pbl* mutants failed to form both the central spindle and the F-actin ring (Table 3 and Figure 5C). Instead of a robust and well-organized central spindle (Figures 2 and 3), these mutant ana-telophases displayed only sparse microtubules between the daughter nuclei and did not show any Klp3A accumulation at the center of the cell (Figure 5D).

The formation of a normal anillin ring also requires wild-type function of *dia*. A continuous anillin ring did not form in ana-telophases from *dia* mutants; instead, only patches of anillin were detected at the equator of these cells (Figure 6, A and B). These anillin patches were observed in both early and late telophase figures, suggesting that *dia* mutations affect anillin band formation rather than its stability. Spermatocytes carrying the new *dia* allele identified in our screen also lacked an F-actin ring and failed to form a well-organized central spindle with Klp3A in the middle, consistent with previous studies of other *dia* alleles (Figure 6 and Table 3; Giansanti *et al*., 1998).

Genes Required for Both Central Spindle and F-Actin Ring Assembly

Mutations in five genes, *scapolo* (*scpo*), *celibe* (*cbe*), *james bond* (*bond*), *sauron* (*sau*), and *smeagol* (*sgo*), affected the formation of both the central spindle and the F-actin ring but did not prevent anillin accumulation at the equator of dividing spermatocytes. In Figure 7 we present images illustrating the phenotype of *scpo*; images from the other mutants in this class are shown in the supplemental material section (Figures 1 and 2). Spermatocytes from males mutant for any of these five genes lacked both an organized central spindle and an F-actin ring throughout ana-telophase (Figure 7 and Table 3; Figures 1 and 2 in Supplemental Material), just as those from *pbl* and *dia* mutants (Figures 5 and 6 and Table 3). However, in *scpo*, *cbe*, *bond*, *sau*, and *sgo* mutants, anillin accumulated normally at the equator of late anaphase cells,

Table 2. Abnormal spermatids in cytokinesis-defective mutants

Genotype	No. of spermatids	Percent spermatids (nuclei:nebenkern)					% Abnormal
		2:1	3:1	4:1	>4:1	Irr[a]	
Oregon-R (control)	258	0	0	0	0	0.8	0.8
bns^{Z3021}/bns^{Z3021}	252	39.3	5.6	27.0	0.3	0	72.2
$bond^{Z0165}/bond^{Z0165}$	213	12.2	1.9	80.3	3.3	0	97.7
$bond^{Z5274}/bond^{Z5274}$	222	19.0	0	75.0	0	0	94.0
$bond^{Z0165}/Df(3R)hh$	184	10.9	0	86.9	0	0	97.8
$bond^{Z5274}/Df(3R)hh$	220	14.6	0	81.8	0	0	96.4
bru^{Z3358}/bru^{Z3358}	176	28.4	0	63.6	0	0	92.0
bru^{Z0704}/bru^{Z0704}	187	39.6	1.1	26.7	2.7	0	70.0
$bru^{Z3358}/Df(2L)pr2b$	244	67.6	3.7	16.0	0.8	0	88.1
cbe^{Z2097}/cbe^{Z2097}	192	14.6	0	80.2	0	0	94.8
cia^{Z2269}/cia^{Z2269}	308	8.4	1.0	84.0	4.0	0	97.4
cia^{Z4674}/cia^{Z4674}	240	33.3	1.7	43.3	0	0	78.3
dia^{Z5930}/dia^{Z5930}	220	3.2	0.4	96.4	0	0	100
dia^{Z4053}/dia^{Z4053}	173	42.8	0.6	12.7	0	0	56.1
$dia^{Z5930}/Df(2L)TW84$	195	1.5	0.5	94.9	0.5	0	97.4
$dia^{Z4053}/Df(2L)TW84$	211	46.0	6.1	10.9	0	0	63.0
fer^{Z5477}/fer^{Z5477}	176	3.4	0	36.9	59.7	0	100
fro^{Z0287}/fro^{Z0287}	248	14.5	1.2	73.4	7.3	1.6	98.0
fro^{Z1497}/fro^{Z1497}	243	17.7	0.4	8.2	0	0	26.3
$fro^{Z1497}/Df(3L)AC1$	271	31.4	1.8	6.6	0.4	2.6	42.8
fwd^{Z0453}/fwd^{Z0453}	117	18.8	0.8	61.5	2.6	4.3	88.0
fws^{Z0161}/fws^{Z0161}	357	16.5	0.6	39.2	5.9	0	62.2
fws^{Z1201}/fws^{Z1201}	236	14.4	3.4	55.1	19.0	0	91.9
$fws^{Z0161}/Df(2L)qua^{1374}$	156	9.0	1.2	10.9	28.9	0	50.0
$fsco^{Z1376}/fsco^{Z1376}$	266	3.0	2.0	87.0	4.0	0	96.0
$fsco^{Z1376}/Df(3R)p25$	206	1.5	0.9	71.4	23.3	0	97.1
fun^{Z1010}/fun^{Z1010}	251	8.0	1.2	89.6	0.4	0	99.0
gio^{Z3934}/gio^{Z3934}	305	19.7	2.3	6.9	0	0	28.9
$gio^{Z3934}/Df(3R)Dl\text{-}Bx12$	230	10.4	0	34.8	0	0	45.2
omt^{Z4144}/omt^{Z4144}	302	15.9	0	71.5	0	0	87.4
$omt^{Z4144}/Df(3R)e^{F1}$	292	12.3	0	78.8	1	0	92.1
onr^{Z4840}/onr^{Z4840}	215	8.0	2.0	75.0	15.0	0	100
$onr^{Z4840}/Df(3R)Espl1$	185	13.0	0	37.8	18.9	0	69.7
pbl^{Z4836}/pbl^{Z4836}	224	9.8	0.9	88.9	0	0	99.6
$pbl^{Z4836}/Df(3L)pbl\text{-}NR$	214	6.5	0	93.5	0	0	100
sau^{Z2217}/sau^{Z2217}	249	0.4	0.4	96.0	2.4	0	99.2
$scpo^{Z2775}/scpo^{Z2775}$	237	7.6	0	86.1	0.8	5.5	100
sgo^{Z1610}/sgo^{Z1610}	216	23.6	2.8	13.9	0	0	40.3
sgo^{Z0742}/sgo^{Z0742}	354	20.1	0.8	28.5	0.3	0	49.7
$sgo^{Z1610}/Df(3R)mbc\text{-}R1$	170	23.5	0	29.4	0	0	52.9

[a] Irr, irregular, refers to spermatids with nuclei of abnormal sizes.

forming a circumferential band indistinguishable from that seen in wild type (Figure 7, B and C, and Table 3; Figure 2 in Supplemental Material). This anillin band, unlike that of wild type (Figure 2), failed to constrict properly during telophase (Figure 7 and Figure 2 in Supplemental Material). Most late telophases from these five mutants displayed anillin rings that were either unconstricted or only poorly constricted. In these rings, anillin was usually more diffuse than in wild type (Figure 7 and Figure 2 in Supplemental Material), suggesting that proper morphology of a late telophase anillin ring depends on the presence of a normal actin ring. These observations confirm that anillin concentration at the equatorial cortex occurs independently of either central spindle or actin ring assembly (Giansanti *et al*., 1999) and suggest that constriction of the anillin ring may normally be driven by constriction of the F-actin ring.

Genes Required for F-Actin Ring Constriction and Central Spindle Stability

Ten genes, *four score* (*fsco*), *brunelleschi* (*bru*), *ciambella* (*cia*), *four way stop* (*fws*), *frodo* (*fro*), *funnel cakes* (*fun*), *omelette* (*omt*), *onion rings* (*onr*), *four wheel drive* (f*wd*), and *giotto* (*gio*) are primarily required for constriction of the F-actin ring (Figures 8 and 9 and Table 3). Spermatocytes from *bru*, *cia*, *fro*, *fsco*, *fun*, *fws*, *omt*, and *onr* displayed similar abnormalities in their cytokinetic structures. We present images from *fsco* spermatocytes to illustrate phenotypes typical for this class of mutants (Figures 8–10); images from *bru*, *cia*, *fro*, *fun*, *fws*, *omt*, and *onr* mutants are shown in the Supplemental Material (Figures 3 and 4) and in Farkas *et al.* (2003). A normal-looking actin ring assembled in *fsco* spermatocytes during early telophase (Figure 8A and Table 3). However, in most mid- and late telophase cells of this mutant, the actin ring was either as large as in early telophase or was only slightly constricted (Figure 8B and Table 3). In addition, in many late telophase figures the poorly constricted actin ring either seemed broken into several pieces or consisted of what seemed to be remnants of the early telophase ring (Figure 8C and Table 3). *fsco* early telophases also displayed a regular anillin band that precisely colocalized with the actin ring (Figure 9A; our unpublished data); anillin continued to co-

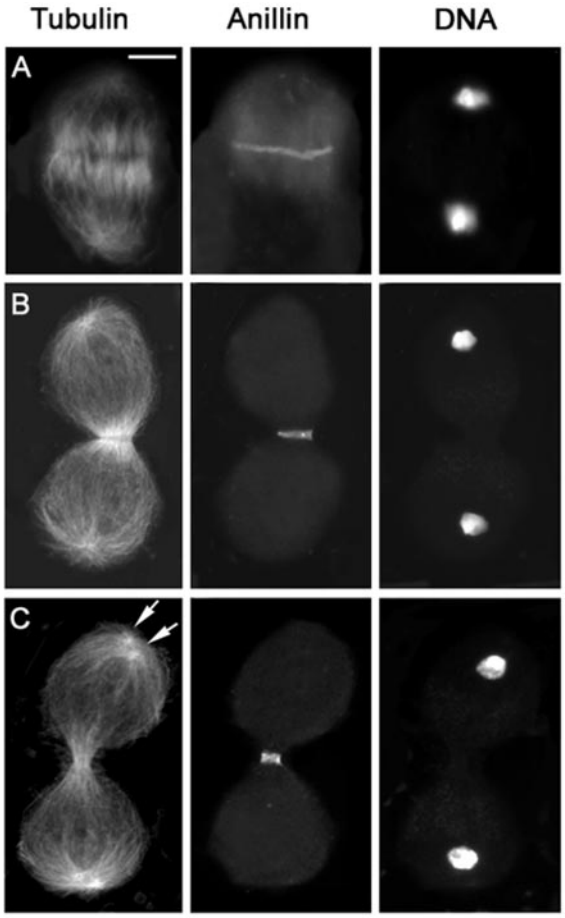

Figure 2. Anillin localization in wild-type primary spermatocytes. Cells are stained for tubulin, anillin, and DNA. (A) Early telophase. (B) Mid-telophase. (C) Late telophase showing aster separation (arrows) at the spindle poles. Bar, 10 μm.

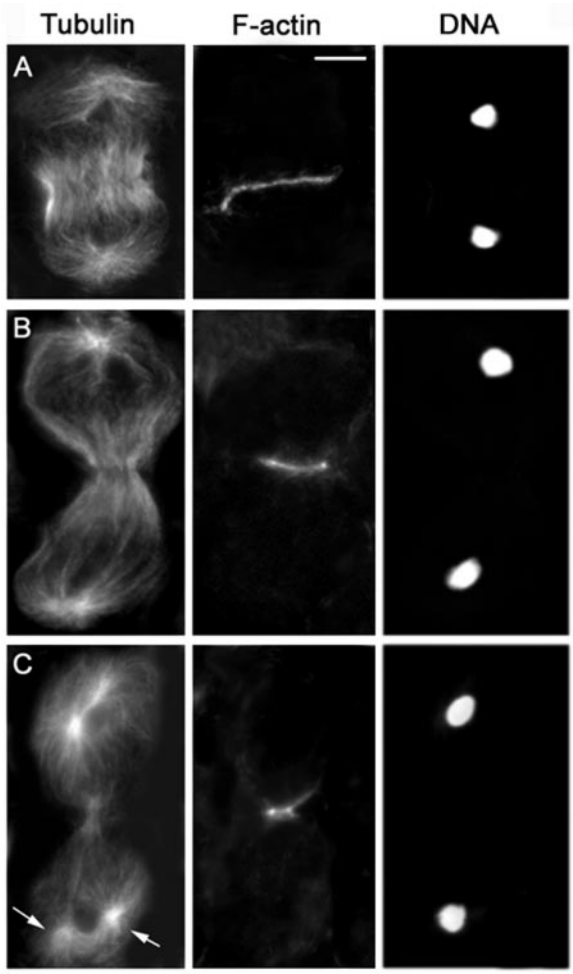

Figure 3. Visualization of the actin ring in wild-type primary spermatocytes. Cells are stained for tubulin, actin, and DNA. (A) Early telophase. (B) Mid-telophase. (C) Late telophase showing aster separation (arrows) at the spindle poles. Bar, 10 μm.

localize with the unconstricted/broken actin ring of *fsco* mutants throughout mid- and late telophase (Figure 9B; our unpublished data).

Spermatocytes from *fsco* mutants also exhibited progressive defects in the central spindle. In most *fsco* early telophases, the central spindle seemed normal and showed normal accumulation of KLP3A at its midzone (Figure 10A and Table 3). However, in mid- and late telophase figures, the central spindle was consistently either less dense than in wild type or completely disorganized (Figures 8–10 and Table 3). Central spindles less robust than their wild-type counterparts showed a reduction in KLP3A concentration at the midzone, whereas disorganized central spindles did not exhibit a detectable KLP3A signal (Fig. 10B). In general, in both *fsco* and the other mutants of its class, the farther a cell had advanced through telophase, the more the central spindle and the actin ring seemed disrupted (Figures 8–10 and Table 3; Figures 3 and 4 in Supplemental Material). In addition, the degree of central spindle abnormality correlated with the degree of actin ring defect. Telophase cells with an intact central spindle showed a complete actin ring, cells with a less robust central spindle tended to have a broken actin ring, and cells without a central spindle displayed only remnants of the contractile ring. Together, our observations indicate that *fsco*, *bru*, *cia*, *fro*, *fun*, *fws*, *omt*, and *onr* spermatocytes have the ability to form both the central spindle and the contractile ring during early telophase. However, as mutant cells progress through telophase, the actin ring fails to constrict properly and the central spindle disassembles.

Examination of living spermatocytes from *fsco*, *bru*, *cia*, *fro*, *fun*, *fws*, *omt*, and *onr* males revealed defective cleavage furrow ingression (Figure 11), as predicted from observation of fixed material. Typical results are presented in Figure 11, showing cytokinesis in *fun* and *fsco* primary spermatocyte over time. In the wild-type ana-telophase cell shown in Figure 11, the furrow advanced over a period of 15 min, leading to the formation of two daughter cells connected by a thin cytoplasmic bridge. In the *fun* and *fsco* cells, after a limited ingression, the furrow regressed, resulting into a clear failure of cytokinesis (Figure 11).

Wild-type functions of *gio* and *fwd* also seem to be required for furrow ingression, but at a later stage than the genes in the *fsco* class. In early telophases and most mid-telophases from *fwd* and *gio* mutants, the central spindle and the contractile ring both seemed normal. However, most *fwd* and *gio* late telophases displayed actin rings that were not fully constricted (Figure 12B and Table 3). In ~10% of these telophases, the unconstricted actin rings were broken and central spindles seemed less dense than in their wild-type counterparts (Table 3). In some late *fwd* and *gio* telophases

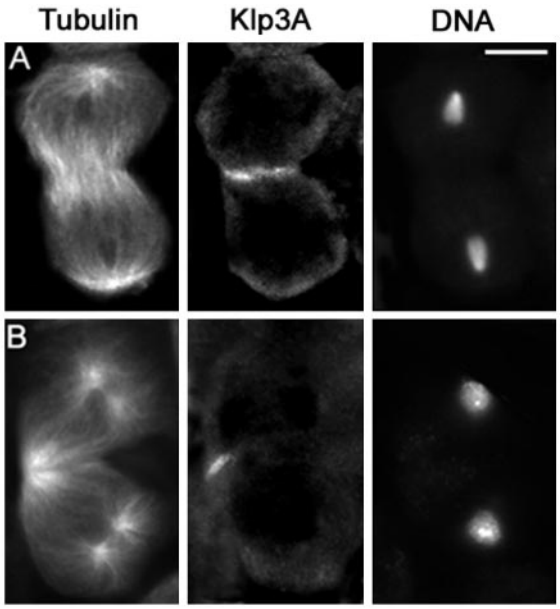

Figure 4. Klp3A localization in wild-type primary spermatocytes. Cells are stained for tubulin, Klp3A, and DNA. (A) Early telophase. (B) Late telophase showing aster separation at the spindle poles. Bar, 10 μm.

displaying a high degree of ring constriction, the F-actin rings seemed thicker than in wild-type cells at the same stage (Figure 12C), as described previously for *fwd* mutants (Brill *et al*., 2000). However, thick actin rings were also seen in some of the rare telophases with constricted rings we occasionally observed in *fsco*, *bru*, *cia*, *fro*, *fun*, *fws*, *omt*, and *onr* mutants. In both *fwd* and *gio* spermatocytes, the anillin band formed normally and constricted to the same extent as the actin ring, as observed in the other mutants of the *fsco* class (our unpublished data).

Genes Required for Actin Ring Disassembly

In spermatocytes from *bird nest soup* (*bns*) mutants, the central spindle had a normal morphology throughout telophase. Both the F-actin and the anillin ring assembled normally and exhibited a normal degree of constriction in mid-telophase cells. However, in late telophase cells, the actin and anillin rings were both abnormal. The actin rings were commonly misshapen, containing excess F-actin compared with wild-type cells at the same stage, and seemed to lack an internal lumen (Figure 13, B and D). We did not detect a clear lumen in 28 actin rings from *bns* late telophases, whereas approximately one-half the wild-type cells at the same stage displayed hollow actin rings. Most anillin rings of *bns* late telophases had a lumen but were more constricted than in wild-type late telophases (Figure 13D). Consistent with the latter observation, ring canals in *bns* spermatids were often smaller than in wild-type (our unpublished data). These results suggest that wild-type function of *bns* may be required for normal disassembly of the actin ring during late telophase.

DISCUSSION

The Mutant Phenotypes Identify Discrete, Genetically Regulated Steps in Spermatocyte Cytokinesis

We have identified 19 genes required for cytokinesis in *Drosophila* spermatocytes, including 16 new loci and additional alleles of *pbl*, *dia*, and *fwd*. Cytological analysis of mutant phenotypes indicated that different genes act at four different major points of the process, defining a stepwise pathway for cytokinesis (Figure 14). Previous studies on spermatocyte cytokinesis identified genes in both the *scpo* class (*chic*, *klp3A*, and *sqh*; Williams *et al*., 1995; Giansanti *et al*., 1998; Giansanti *et al*., 2001a) and the *bns* class (*tsr*; Gunsalus *et al*., 1995; Giansanti *et al*., 1999) but not in either the *pbl/dia* or the *fsco* classes. Studies on *polo* spermatocytes showed that this gene is required for both central spindle and actin ring formation, but they did not determine whether it is also required for anillin localization at the cell equator (Carmena *et al*., 1998; Herrmann *et al*., 1998).

Our results indicate that *pbl* and *dia* are required for the formation of three cytokinetic structures: the anillin equatorial band, the central spindle, and the contractile ring, suggesting that these genes control an early step of cytokinesis required for the assembly of these three structures. Mutations in the five genes of the *scpo* class allow the formation of the anillin band but prevent the assembly of both the central spindle and the contractile ring (Figure 14). Thus, these genes either act later than both *pbl* and *dia*, or act at the same time as *pbl* and *dia* but control only central spindle and actin ring formation without affecting anillin accumulation at the cleavage site. The mutant phenotypes associated with the *scpo* class demonstrate conclusively that formation of the anillin band at the cell cortex can occur independently of assembly of both the central spindle and the F-actin ring, consistent with the observation that the equatorial anillin ring forms before a detectable F-actin ring (Giansanti *et al*., 1999). A subsequent step of spermatocyte cytokinesis is specified by the ten genes in the *fsco* class (Figure 14). These genes are not required for the formation of the anillin equatorial band, the central spindle, or the contractile ring during early telophase, but they are required for proper constriction of the F-actin ring during mid- and late telophase. The *bns* gene acts in a late step of spermatocyte cytokinesis. In *bns* mutant males, the major cytokinetic structures form and the F-actin ring constricts, but disassembly of the constricted ring is defective (Figure 14).

The finding that mutations in 22 different genes (Figure 14) affect only four steps of cytokinesis strongly suggests that these steps represent crucial genetically regulated landmarks in the process. However, because these steps have been defined by examining cells stained only for anillin, tubulin, F-actin, and Klp3A, it cannot be excluded that cytological analysis of mutant spermatocytes immunostained for other proteins involved in cytokinesis will reveal subdivisions within each of these steps.

The Role of pbl and dia in Spermatocyte Cytokinesis

Our results indicate that the wild-type function of *pbl* and *dia* is required for the formation of the anillin equatorial band, the central spindle, and the contractile ring. The finding that mutations in *pbl* and *dia* disrupt both central spindle and contractile ring formation is consistent with the molecular studies on these genes. Recent work has shown that the Rho GTP-exchange factor (Rho GEF) Pebble binds the Rho GTPase activating protein RacGAP50C, which also forms a complex with the kinesin-like protein Pavarotti (Somers and Saint, 2003). These molecular interactions seem to be evolutionary conserved, because the *C. elegans* RacGAP50 orthologue CYK-4 and the Pav orthologue ZEN-4 form a complex, called centralspindlin, which has microtubule bundling activity and is required for central spindle formation (Mishima *et al*., 2002). Because Pbl accumulates at the equatorial cortex and the RacGAP50C–Pav complex at the central spindle

Table 3. Cytological characterization of telophases of cytokinesis-defective mutants

	Early telophase				Mid- and late telophases				
Genotype	No. of cells scored	CS and AR both normal %	CS and AR both defective[a] %	CS and AR both absent %	No. of cells scored	CS and AR both normal %	CS normal, AR abnormal[b] %	CS and AR both defective[a] %	CS and AR both absent %
Oregon-R	64	100	0	0	78	100	0	0	0
bns^{Z3021}/bns^{Z3021}	30	100	0	0	34	40	60	0	0
$bond^{Z0165}/bond^{Z0165}$	30	6	0	94	32	6	0	0	94
$bond^{Z5274}/bond^{Z5274}$	34	12	0	88	60	0	0	0	100
$bond^{Z0165}/Df(3R)hh$	44	9	0	91	38	0	0	0	100
bru^{Z3358}/bru^{Z3358}	57	88	12	0	54	11	0	89	0
$bru^{Z3358}/Df(2L)pr2b$	40	95	5	0	66	14	0	86	0
cbe^{Z2097}/cbe^{Z2097}	40	10	0	90	78	3	0	0	97
cia^{Z4674}/cia^{Z4674}	30	87	13	0	32	3	0	97	0
dia^{Z5930}/dia^{Z5930}	47	9	0	91	48	0	0	0	100
$dia^{Z5930}/Df(2L)TW84$	34	0	0	100	54	0	0	0	100
fro^{Z0287}/fro^{Z0287}	31	87	13	0	54	26	29	39	6
$fsco^{Z1376}/fsco^{Z1376}$	33	94	6	0	30	13	0	80	7
$fsco^{Z1376}/Df(3R)p25$	55	87	13	0	49	10	0	90	0
$fwd^{Z0453}/Df(3L)7C$	30	100	0	0	46	36	55	9	0
fws^{Z0161}/fws^{Z0161}	39	95	5	0	34	15	0	85	0
$fws^{Z0161}/Df(2L)qua^{1374}$	44	100	0	0	38	8	0	92	0
fun^{Z1010}/fun^{Z1010}	55	95	5	0	74	7	0	93	0
gio^{Z3934}/gio^{Z3934}	35	100	0	0	42	46	47	7	0
$gio^{Z3934}/Df(3R)Dl\text{-}Bx12$	32	100	0	0	37	38	43	19	0
omt^{Z4144}/omt^{Z4144}	44	93	7	0	40	20	0	75	5
$omt^{Z4144}/Df(3R)e^{F1}$	27	85	15	0	36	11	0	83	6
onr^{Z4840}/onr^{Z4840}	30	70	30	0	35	3	0	72	25
$onr^{Z4840}/Df(3R)Espl1$	32	84	16	0	33	3	0	76	21
pbl^{Z4836}/pbl^{Z4836}	63	5	0	95	87	0	0	0	100
$pbl^{Z4836}/Df(3L)pbl\text{-}NR$	35	0	0	100	42	0	0	0	100
sau^{Z2217}/sau^{Z2217}	35	11	0	89	43	3	0	3	94
$scpo^{Z2775}/scpo^{Z2775}$	30	3	0	97	39	10	0	0	90
sgo^{Z1610}/sgo^{Z1610}	32	31	0	69	35	20	0	0	80
$sgo^{Z1610}/Df(3R)mbc\text{-}R1$	28	29	0	71	44	9	0	0	91

AR, actin ring; CS, central spindle.

[a] Cells contain barely constricted ARs, large broken ARs, or AR fragments, and display CSs less dense than in wild type.

[b] In *bns* the AR is misshaped and contains excess of F-actin; in *fro*, *fwd*, and *gio* the ARs are either unconstricted or poorly constricted.

midzone, it has been suggested that interactions between Pbl and RacGAP50 could result in local activation of Rho1, which may in turn trigger a cascade of events leading to the formation of the contractile ring (Somers and Saint, 2003). One of the downstream targets of activated Rho1 is the Diaphanous formin homology protein, which is known to interact with both microtubules and the actin cytoskeleton (Palazzo *et al*., 2001).

Our findings also indicate that wild-type functions of *pbl* and *dia* are required for proper anillin accumulation at the equatorial cortex of spermatocytes. However, although there was no detectable anillin concentration at the cortex of *pbl* mutants, anillin accumulated at the cell equator of *dia* mutants examined but failed to form a continuous ring. The phenotypical differences between *pbl* and *dia* mutants are likely to reflect different gene functions rather than result from partial loss of function of the *dia* allele used for phenotypical characterization ($dia^{Z5930)}$). Males homozygous for dia^{Z5930} and $dia^{Z5930}/Df(2L)TW84$ hemizygotes displayed very similar frequencies of both aberrant spermatids (Table 2) and abnormal telophases (Table 3), suggesting that the dia^{Z5930} allele is functionally null in the male germline. Thus, although *pbl* and *dia* are both required for proper anillin accumulation at the cell equator and have been included in the same functional class for sake of simplicity (Figure 14), they seem to control different steps of the process that leads to the formation of the anillin ring.

These observations, together with the fact that anillin marks the cleavage site before actin ring assembly, raise the question of the role of anillin during spermatocyte cytokinesis. Studies on S2 tissue culture cells have shown that anillin depletion by RNA interference (RNAi) neither affects central spindle assembly nor actin ring formation and its initial constriction. However, in the absence of anillin, late telophase cells exhibit abnormally shaped actin rings and membrane protrusions at the cleavage site, suggesting that anillin regulates membrane-contractile ring interactions during late stages of cytokinesis. Thus, the phenotype of anillin-depleted S2 cells suggests that anillin accumulation at the spermatocyte equator is not required for actin ring assembly and constriction. However, observation of anillin behavior in spermatocytes and S2 cells raises the possibility that this protein may play different roles in the two cell types. In S2 cells, and in other mitotic cells such as neuroblasts and ganglion mother cells, anillin and actin progressively concentrate at the equatorial cortex of late telophases, forming wide bands that largely overlap both temporally and spatially (Giansanti *et al*., 2001b; Somma *et al*., 2002). As cell

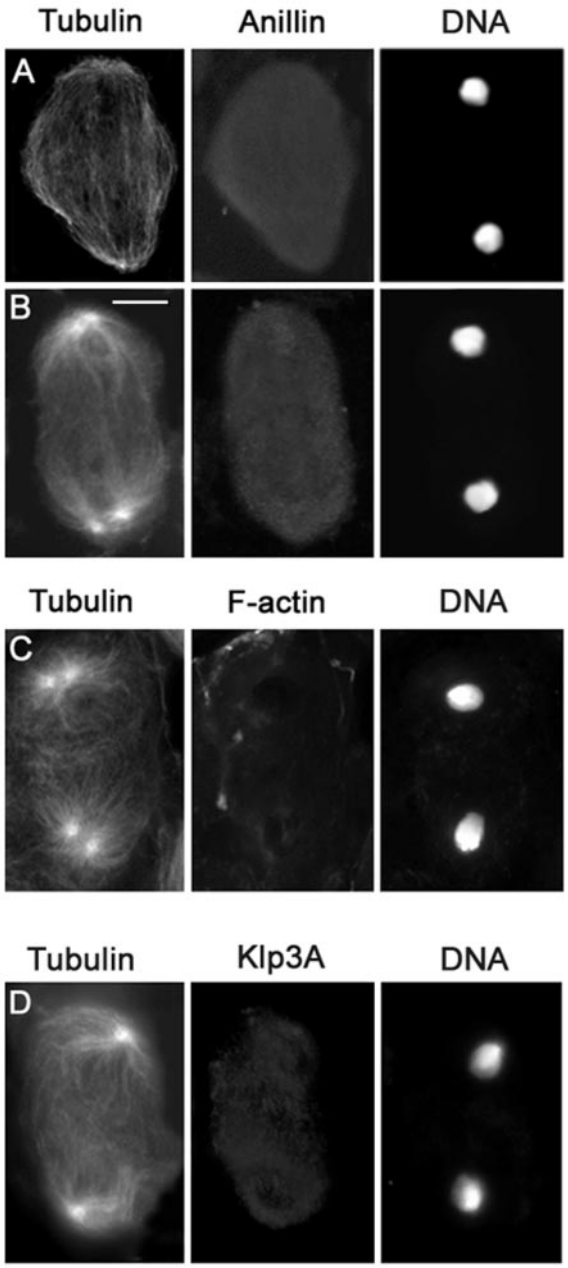

Figure 5. Cytological phenotype of *pbl* mutant spermatocytes. Cells are stained for tubulin, DNA, and either anillin, actin, or Klp3A. (A and D) Early telophases. (B and C) Late telophases. Note the absence of an organized central spindle with Klp3A at its midzone, the anillin equatorial band, and the actin ring. Bar, 10 μm.

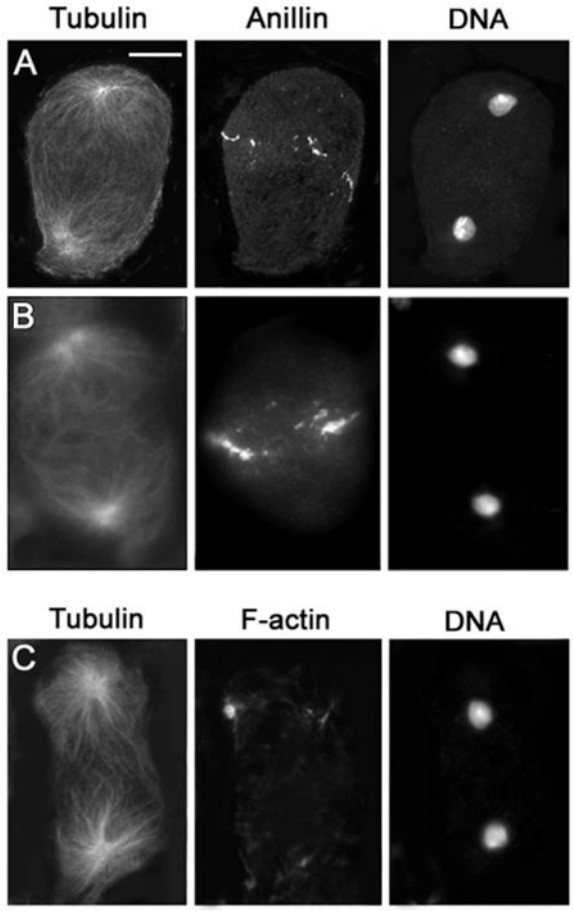

Figure 6. Cytological phenotype of *dia* mutant spermatocytes. Cells are stained for tubulin, DNA and either anillin or actin. (A) Early telophase. (B) Late telophase. (C) Mid-telophase. Note the discontinuity of the anillin band and the absence of both the contractile ring and an organized central spindle. Bar, 10 μm.

division proceeds, these bands progressively narrow, until they form a thin contractile ring in which actin and anillin precisely colocalize. In contrast, in late anaphase spermatocytes anillin abruptly concentrates in a narrow equatorial band (Figure 2). Shortly afterward, these cells form a narrow actin ring that exactly colocalizes with the anillin band (Giansanti *et al*., 1998). The reasons for the different dynamic behavior of anillin and actin during spermatocyte and somatic cell cytokinesis are not understood, but they may reflect different mechanisms of cell cleavage in different cell types. For example, the abrupt concentration of anillin at the spermatocyte equator may reflect an early requirement of this protein to control proper membrane behavior at the cleavage site. Spermatocytes are indeed much larger than somatic cells and may require formation of new membrane for furrow ingression beginning with the early stages of cytokinesis. In summary, failure of proper anillin accumulation at spermatocyte equator may not affect the early steps of cytokinesis, impairing only membrane–ring interactions at the end of the process. Alternatively, local accumulation of anillin may be required at the onset of cytokinesis for furrow ingression. Although we favor the second possibility, our results do not allow discrimination between the two alternatives. Definition of the role of anillin during meiotic cytokinesis of *Drosophila* males must await phenotypical analysis of spermatocytes from *anillin* mutants.

Relationships between the Central Spindle and the Contractile Ring

We have characterized the cytological phenotype of mutants in 18 genes required for spermatocyte cytokinesis. Seven of these mutants (*pbl*, *dia*, *scpo*, *bond*, *cbe*, *sau*, and *sgo*) fail to assemble both a central spindle and a contractile ring; 11 mutants allow the formation of both structures but are either defective in ring constriction (*fsco*, *bru*, *cia*, *fro*, *fun*, *fwd*, *fws*, *gio*, *omt*, and *onr*) or in ring disassembly (*bns*). These results establish a strong correlation between central spindle and

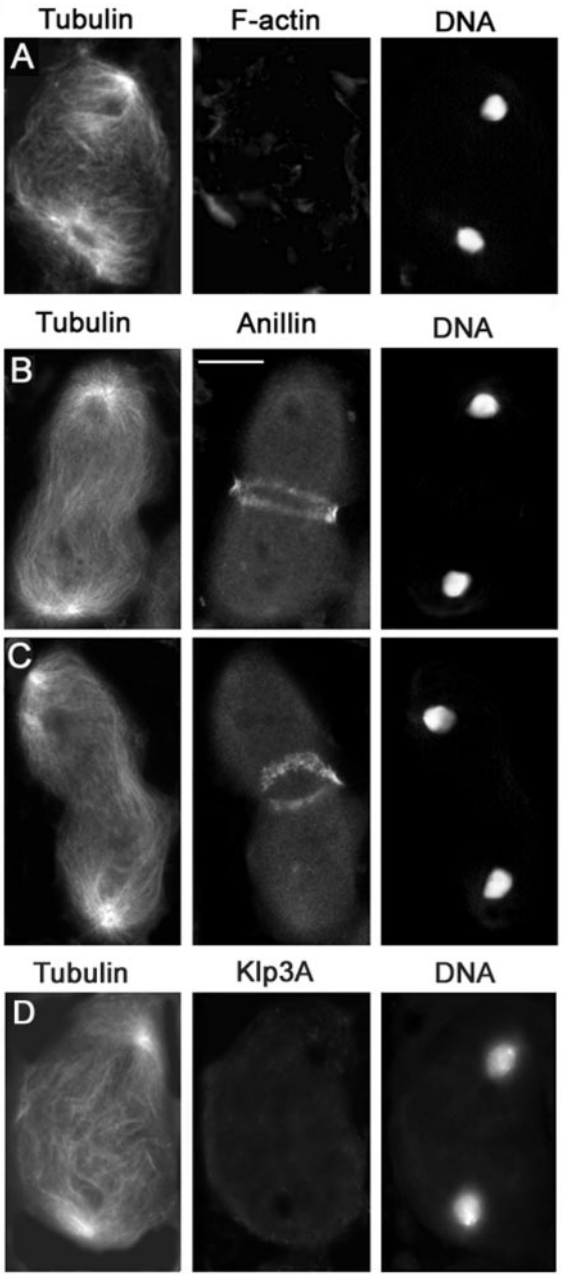

Figure 7. Cytological phenotype of *scpo* mutant spermatocytes. Cells are stained for tubulin, DNA, and either anillin, actin, or Klp3A. (A) Late telophase lacking both an organized central spindle and the actin ring. (B and C) Late telophases with severely defective central spindles, displaying unconstricted (B) or poorly constricted anillin bands (C). Note that these anillin bands are more diffuse than in wild-type. (D) Mid-telophase laking an organized central spindle and Klp3A accumulation at the center of the cell. Bar, 10 μm.

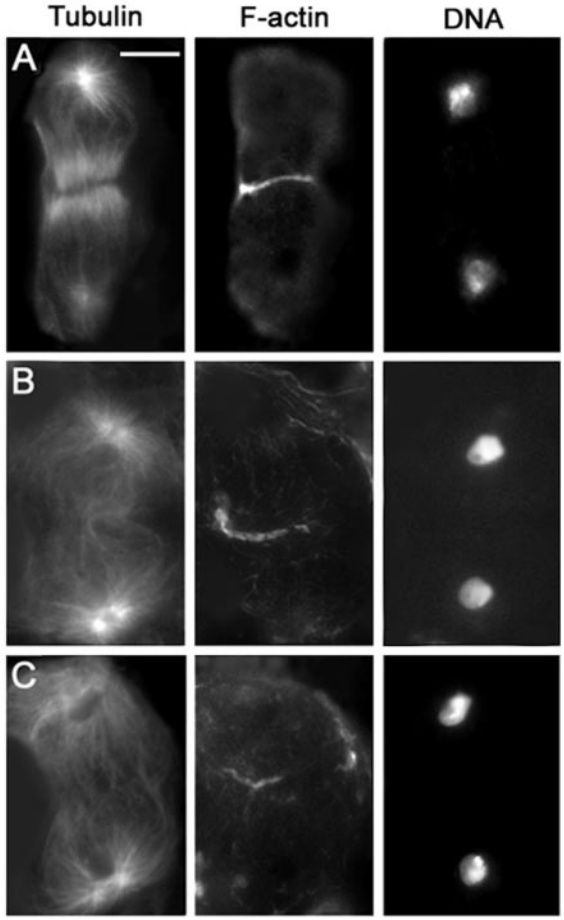

Figure 8. Cytological phenotype of *fsco* mutant cells. Cells are stained for tubulin, DNA, and actin. (A) *fsco* mid-telophase with a normal central spindle and a regular actin ring. (B and C) Late telophases displaying unconstricted (B) and broken (C) actin rings and severely defective central spindles. Bar, 10 μm.

contractile ring assembly, consistent with an interdependence of these structures (Giansanti *et al*., 1998; Somma *et al*., 2002).

Previous studies (Giansanti *et al*., 1998; Somma *et al*., 2002) and observations on mutants of the *pbl/dia* and *scpo* classes indicate that a cooperative interaction between the central spindle and the contractile ring is necessary for assembly of both structures during the initial stages of cytokinesis. The cytological analysis of mutants in the *fsco* class demonstrates for the first time that these structures are mutually dependent also at later stages of the cytokinetic process. We have shown that in these mutants both the central spindle and the contractile ring assemble normally. In mutant late telophases, however, both the central spindle and the contractile ring often seem severely defective or altogether absent. Notably, the degree of central spindle abnormality always correlated with the degree of actin ring defect in late telophase cells. This observation suggests that the stability of both the central spindle and the contractile ring requires continuous interactions between these structures throughout cytokinesis. It is likely that failures in ring constriction in the *fsco* class mutants reduce these central spindle–ring interactions, leading to defects in both structures.

Although all the extant results indicate that the central spindle and the contractile ring are mutually dependent structures in *Drosophila* cells, this is not true for all animal cells. A limited number of studies strongly suggest that the central spindle and the contractile ring are also interdependent structures in mammalian somatic cells (Cao and Wang, 1996; Fishkind *et al*., 1996). In contrast, studies on *C. elegans* one-cell embryos clearly showed that the central spindle and the contractile ring can assemble independently. However, these studies also showed that proper organization of central spindle is essential for completion of cytokinesis (Pow-

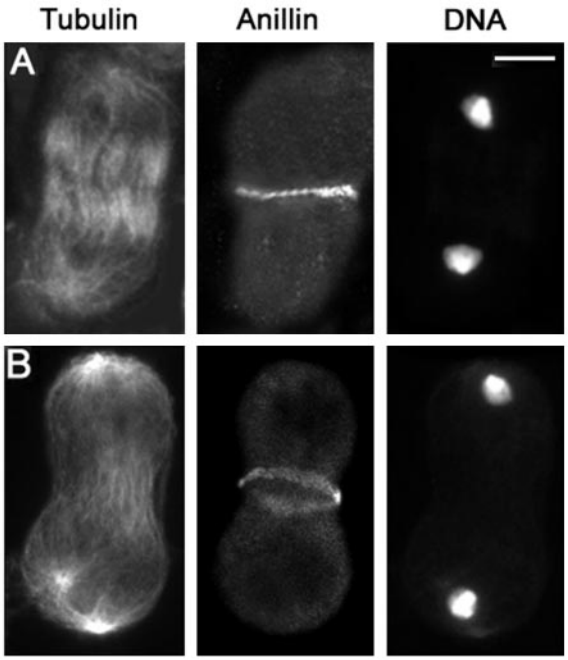

Figure 9. Anillin localization in *fsco* mutant spermatocytes. Cells are stained for tubulin, DNA and anillin. (A) Early *fsco* telophase with a normal anillin band. (B) Late telophase with a poorly constricted anillin band and a severely defective central spindle. Bar, 10 μm.

ers *et al*., 1998; Raich *et al*., 1998; Jantsch-Plunger *et al*., 2000). The differences between *Drosophila* and *C. elegans* may be due to the different geometry of dividing cells. In *Drosophila* and mammalian cells, the central spindle assembles close to the equatorial cortex. In contrast, in the large *C. elegans* one-cell embryo the central spindle forms in the center of the cell at a considerable distance from the cortex. It is thus possible that *C. elegans* cytokinesis consists of two steps. In a first step, the central spindle and the contractile ring assemble independently in distant cellular areas and the cleavage furrow ingression begins. The second step would take place when the central spindle and the contractile ring have come into contact and could involve central spindle–contractile ring interactions similar to those that occur in *Drosophila* cells.

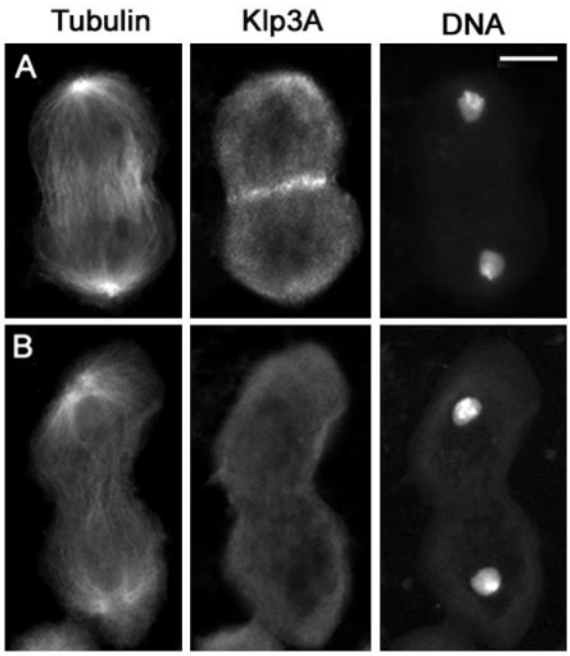

Figure 10. Klp3A localization in *fsco* mutant spermatocytes. Cells are stained for tubulin, DNA, and Klp3A. (A) Early *fsco* telophase with a normal Klp3A signal at the central spindle midzone. (B) Late telophase with a severely defective central spindle and no Klp3A accumulation at the center of the cell. Bar, 10 μm.

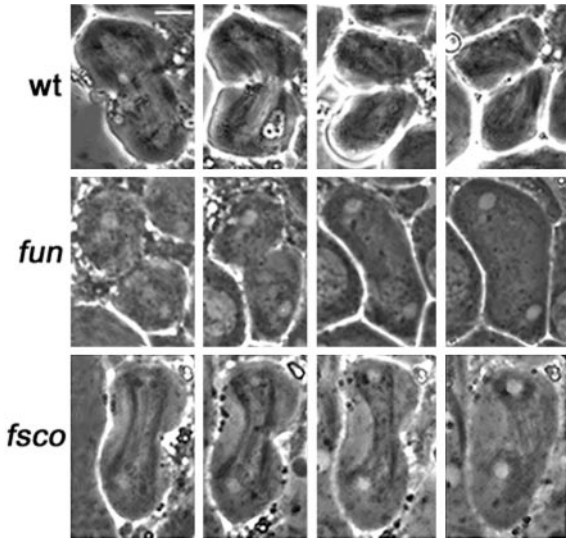

Figure 11. In vivo time course of cleavage furrow in living spermatocytes under oil. Panels in each set are consecutive images taken at 5-min intervals. In wild type (wt), a furrow is initiated ~10 min after anaphase onset (left panel of the set) and continues to progress through the time course. In the *fun* and *fsco* mutants, the furrow also initiates ~10 min after anaphase onset but shows a limited ingression and then regresses leading to a failure of cytokinesis. Bar, 10 μm.

We do not currently understand the molecular basis of the interdependence between the central spindle and the contractile ring. The formation and maintenance of both of these structures could be mediated by physical interactions between central spindle microtubules and components of the contractile ring. For example, as mentioned earlier, interactions between the centralspindlin component RacGap50C and the cortically located Pbl could activate Rho1 (Somers and Saint, 2003), which would in turn activate Dia, leading to both contractile ring formation and central spindle stabilization. Alternatively, the central spindle and the contractile ring could be coupled by a checkpoint-like regulatory mechanism that prevents the formation of either structure when the other is not properly assembled. Whatever the mechanism of the central spindle–contractile ring mutual dependence, it must involve the functions of the genes in the *scpo* class. Hence, we are confident that the molecular analysis of these genes will provide further insight into the mechanisms underlying central spindle–contractile ring interactions.

Regulation of the Actomyosin Ring Constriction and Disassembly

The genes identified by mutations in *fsco*, *bru*, *cia*, *fro*, *fun*, *fwd*, *fws*, *gio*, *omt*, and *onr* are primarily required for constriction of the actomyosin ring and cleavage furrow ingression.

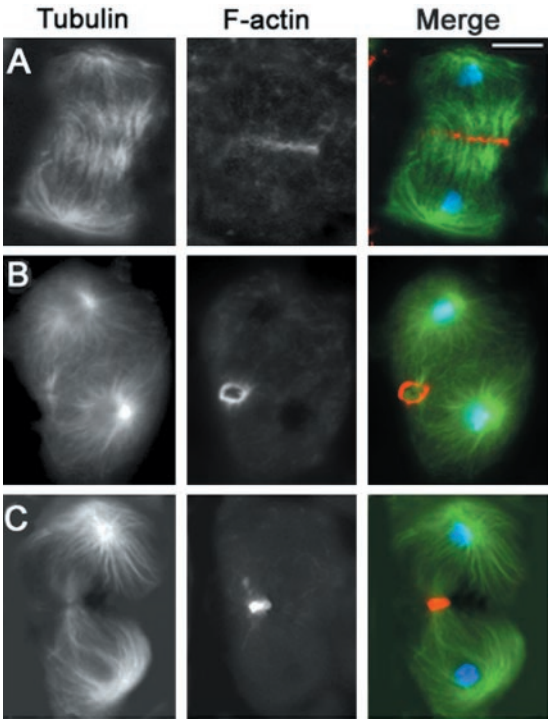

Figure 12. Defects in ring morphology in telophases from *fwd* mutants. Cells are stained for tubulin (green), actin (orange), and DNA (blue). (A) Early mutant telophase showing a regular actin ring. (B) Late telophase with an incompletely constricted actin ring. (C) Mutant late telophase with a constricted, thick ring. Bar, 10 μm.

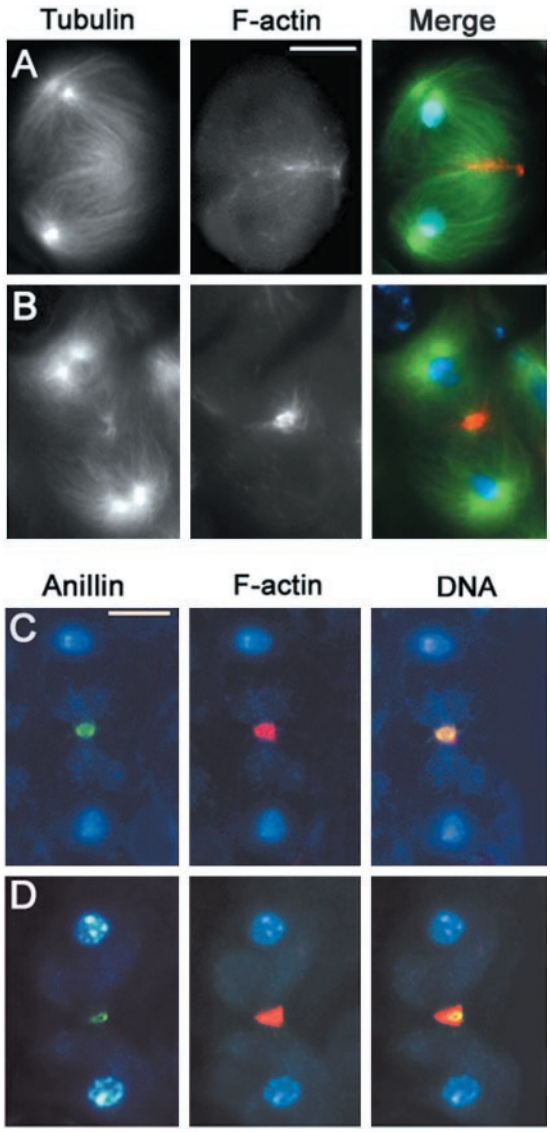

Figure 13. Cytological phenotype of *bns* mutants. The cells shown in A and B are stained for tubulin (green), actin (orange), and DNA (blue); the telophases shown in C and D are stained for anillin (green), actin (red), and DNA (blue). (A) Mid-telophase with a normal actin ring and a regular central spindle. (B) Late telophase with an abnormally large actin mass surrounding the midbody. (C) Wild-type late anaphase showing colocalization of actin and anillin in the contractile ring. (D) *bns* late telophase showing an overconstricted anillin ring embedded into a large mass of F-actin. Bar, 10 μm.

The *fwd* and *fws* genes have been characterized at the molecular level; respectively, they encode a phosphatidylinositol 4-kinase and the Cog5 subunit of the conserved oligomeric Golgi complex (Brill *et al*., 2000; Farkas *et al*., 2003). Recent work has shown that *gio* encodes a *Drosophila* phosphatidylinositol transferase (Giansanti, Bonaccorsi, Kurek, Farkas, Fuller, and Gatti, unpublished data). Studies on the biochemical roles of phosphatidylinositol transferase, phosphatidylinositol 4-kinase, and the conserved oligomeric Golgi complex indicate that these proteins are involved in the formation and trafficking of Golgi-derived vesicles (Allen-Baume *et al*., 2002; De Matteis at al., 2002; Ungar *et al*., 2002). Delivery of Golgi-based vesicles to the plasma membrane and their fusion with preexisting membrane is thought to be one of the main mechanisms of new membrane formation, and several studies indicate that membrane addition at the ingressing furrow occurs by this mechanism (Byers and Armstrong, 1986; Aimar, 1997; Skop *et al*., 2001; Shuster and Burgess, 2002). Mutations in *fwd*, *fws*, and *gio* could thus disrupt membrane addition to the cleavage furrow. The finding that other mutants in the *fsco* class have a similar phenotype to *fwd*, *fws*, and *gio* suggests that these mutants may be defective in the same process. Our observations on fixed material have shown that the mutants in the *fsco* class display late telophases with poorly constricted actin rings. In addition, in vivo analysis has shown that in the same mutants the cleavage furrow ingresses to a limited extent, and then regresses. Together, these findings suggest that proper membrane addition to the equator of dividing spermatocytes is not essential for either contractile ring assembly or its initial constriction but it is required for continuation and completion of ring constriction.

A new gene required for actin ring disassembly was also identified in the screen. Late telophase spermatocytes from *bns* mutants display misshapen and large actin rings that lack an internal lumen. This suggests that in these mutants, the contractile ring fails to disassemble at the end of cell division and accumulates abnormally high amounts of F-actin. The *bns* phenotype is very similar to that observed in mutants in the *twinstar* gene, which encodes *Drosophila* cofilin (Gunsalus *et al*., 1995). Cofilins are small actin-binding proteins that sever actin filaments and promote F-actin depolymerization (Bamburg *et al*., 1999). The *bns* gene may encode another actin-severing protein or a factor that activates cofilin. Alternatively, the *bns* gene product could fa-

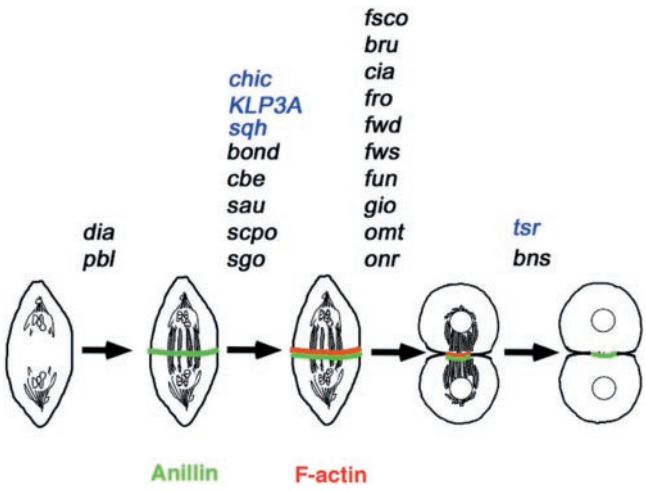

Figure 14. Genetic control of spermatocyte cytokinesis. The genes required for the accomplishment of each step of cytokinesis are above the arrows. Genes depicted in black have been identified and/or characterized in the present study; those depicted in blue have been described in previous reports (see text for further explanation).

cilitate F-actin disassembly by another mechanism, for example, by sequestering actin monomers.

The Cell Type-specific Control of Drosophila Cytokinesis

Growing evidence suggests that cell type-specific control of cytokinesis may be a common phenomenon in metazoans. For example, studies on mouse have shown that the Rho-dependent citron kinase is required for cytokinesis in both neuroblasts and male gonial cells but not in other cell types (Di Cunto *et al*., 2000). However, this important aspect of eukaryotic cell division has not been widely addressed. Most studies on cytokinesis have been carried out in single-celled organisms such as yeast, or in single-cell types of multicellular organisms, such as the one-cell embryo of *C. elegans* or mammalian tissue culture cells. The collection of *Drosophila* mutants isolated in our screen provides a unique tool to address questions about cell type-specific control mechanisms for cytokinesis. Data from our screen and previous studies suggest that meiotic cytokinesis in *Drosophila* males is governed by two categories of genes: those required for both mitotic and meiotic cytokinesis, and those specifically required for spermatocyte cytokinesis.

Our screen identified viable mutations in 19 genes required for cytokinesis of *Drosophila* spermatocytes, including alleles of *dia*, *fwd*, and *pbl*. Previous studies have described lethal mutations of *pbl* that affect embryonic cell cytokinesis (Hime and Saint, 1992; Lehner, 1992; Prokopenko *et al*., 1999) and have demonstrated that *pbl* ablation by RNAi disrupts cytokinesis in S2 tissue culture cells (Somma *et al*., 2002). Previously identified mutations in *dia* include lethal alleles affecting both neuroblast and spermatocyte cytokinesis and homozygous-viable, male sterile alleles that disrupt meiotic cytokinesis (Castrillon and Wasserman, 1994). These results indicate that *dia* and *pbl* are required for both mitotic cytokinesis and meiotic cytokinesis in males.

In contrast, null mutations in the broadly expressed *fwd*, *fws*, and *klp3A* genes disrupt spermatocyte cytokinesis but have no observable effect on larval neuroblast mitosis (Williams *et al*., 1995; Brill *et al*., 2000; Farkas *et al*., 2003; Giansanti, Bonaccorsi, and Gatti, unpublished data). In addition, depletion of either Fwd, Fws, or Klp3A by RNAi did not block cytokinesis in S2 cultured cells (Somma *et al*., 2002; Giansanti and Somma, unpublished data). Thus, wild-type functions of *fwd*, *fws*, and *klp3A* are essential for spermatocyte cytokinesis but do not seem to be required for mitotic cytokinesis. The products of these broadly expressed genes may play similar functions in meiotic and somatic cell cytokinesis but spermatocytes may be more sensitive than somatic cells to disruptions in their function.

In a separate study, we have identified *gio* lethal alleles that disrupt cytokinesis in larval neuroblasts (Giansanti, Bonaccorsi, Kurek, Farkas, Fuller, and Gatti, unpublished data), indicating a general requirement of this gene for *Drosophila* cytokinesis. The remaining 14 genes (*bns*, *bond*, *bru*, *cbe*, *cia*, *fer*, *fro*, *fsco*, *fun*, *omt*, *onr*, *sau*, *scpo*, and *sgo*) identified by our screen are specified by mutations that disrupt cytokinesis of most meiotic divisions (Table 2) but do not seem to affect mitotic cytokinesis of larval neuroblasts (our unpublished data). Some of these mutations could be in genes whose products are specifically required for meiotic cytokinesis in males. Other mutations could be lesions in genes required for both meiotic and mitotic cytokinesis. These lesions, however, could be in spermatocyte-specific promoters/enhancers or exons, eliminating the gene product in meiotic cells but not in somatic tissues. Our current results do not allow us to distinguish among these alternatives for any of the 14 genes. Determination of the roles of these genes during mitotic and meiotic cytokinesis will require isolation and characterization of additional mutant alleles, as well as studies aimed at defining the molecular lesions of the mutations and the patterns of gene expression.

ACKNOWLEDGMENTS

We are extremely grateful to Charles Zuker in whose laboratory, and with whose unfailing support, the isolation and the preliminary cytological characterizations of the male-sterile mutations described in this article were carried out. We also thank Chris Field for the anti-anillin antibody; Christina Chan, Ajnia Rivera, Cricket Wood, and Benjamen Bolival for assisting with the mapping experiments; and Carmen Robinett and Todd Blankenship for many discussions. This work was supported by grants from Fondo per gli Investimenti della Ricerca di Base (RBNE01KXC9-004), Progetto Strategico Genomica Funzionale (L449/97), and Centro di Eccellenza di Biologia e Medicina Molecolare (to M.G.); by National Institutes of Health training grant ZT52GM07790 (to R.M.F.) and National Institutes of Health grant IRD-IGM62276 (to M.T.F.); and by National Science Foundation grants HRD962704 and DCB0211733 (to B.T.W.).

REFERENCES

Adams, R.R., Tavares, A.A., Salzberg, A., Bellen, H.J., and Glover, D.M. (1998). *pavarotti* encodes a kinesin-like protein required to organize the central spindle and contractile ring for cytokinesis. Genes Dev. *12*, 1483–1494.

Aimar, C. (1997). Formation of new plasma membrane during the first cleavage cycle in the egg of *Xenopus laevis*: an immunocytological study. Dev. Growth Differ. *39*, 693–704.

Allen-Baume, V., Segui, B., and Cockcroft, S. (2002). Current thoughts on the phosphatidylinositol transfer protein family. FEBS Lett. *531*, 74–80.

Bamburg, J.R., McGough, A., and Ono, S. (1999). Putting a new twist on actin: ADF/cofilins modulate actin dynamics. Trends Cell Biol. *9*, 364–370.

Brill, J.A., Hime, G.R., Scharer-Schuksz, M., and Fuller, M.T. (2000). A phospholipid kinase regulates actin organization and intercellular bridge formation during germline cytokinesis. Development *127*, 3855–3864.

Byers, T.J., and Armstrong, P.B. (1986). Membrane protein redistribution during *Xenopus* first cleavage. J. Cell Biol. *102*, 2176–2184.

Cao, L.-G. and Wang, Y.-L. (1996). Signals from the spindle midzone are required for the stimulation of cytokinesis in cultured epithelial cells. Mol. Biol. Cell *7*, 225–232.

Carmena, M., Riparbelli, M.G., Minestrini, G., Tavares, A.M., Adams, R., Callaini, G., and Glover, D.M. (1998). *Drosophila* polo kinase is required for cytokinesis. J. Cell Biol. *143*, 659–671.

Castrillon, D.H., and Wasserman, S.A. (1994). Diaphanous is required for cytokinesis in *Drosophila* and shares domains of similarity with the products of the limb deformity gene. Development *120*, 3367–3377.

Cenci, G., Bonaccorsi, S., Pisano, C., Vernì, F., and Gatti, M. (1994). Chromatin and microtubule organization during premeiotic, meiotic and early postmeiotic stages of *Drosophila melanogaster* spermatogenesis. J. Cell Sci. *10*, 3521–3534.

Cooley, L., Verheyen, E., and Ayers, K. (1992). *chickadee* encodes a profilin required for intercellular cytoplasm transport during *Drosophila* oogenesis. Cell *69*, 173–184.

De Matteis, M., Godi, A., and Corda, D. (2002). Phosphoinositides and the Golgi complex. Curr. Opin. Cell Biol. *14*, 434–447.

Di Cunto, F., *et al*. (2000). Defective neurogenesis in citron kinase knockout mice by altered cytokinesis and massive apoptosis. Neuron *28*, 115–127.

Farkas, R.M., Giansanti, M.G., Gatti, M., and Fuller, M.T. (2003). The *Drosophila* Cog5 homologue is required for cytokinesis, cell elongation, and assembly of specialized Golgi architecture during spermatogenesis. Mol. Biol. Cell *14*, 190–200.

Field, C., and Alberts, B.M. (1995). Anillin, a contractile ring protein that cycles from the nucleus to the cell cortex. J. Cell Biol. *131*, 165–178.

Fishkind, D.J., Silverman, J.D., and Wang, Y.-L. (1996). Function of spindle microtubules in directing cortical movements and actin filaments organization in dividing cultured cells. J. Cell Sci. *109*, 2041–2051.

Fuller, M. (1993). Spermatogenesis. In: Development of *Drosophila*, ed. A. Martinez-Arias and M. Bate, Cold Spring Harbor, NY: Cold Spring Harbor Laboratory Press, 71–147.

Gatti, M., Giansanti, M.G., and Bonaccorsi, S. (2000). Relationships between the central spindle and the contractile ring during cytokinesis in animal cells. Microsc. Res. Tech. *49*, 202–208.

Giansanti, M.G., Bonaccorsi, S., Bucciarelli, E., and Gatti, M. (2001a). *Drosophila* male meiosis as a model system for the study of cytokinesis in animal cells. Cell Struct. Funct. *26*, 631–639

Giansanti, M.G., Bonaccorsi, S., and Gatti, M. (1999). The role of anillin in meiotic cytokinesis of *Drosophila* males. J. Cell Sci. *112*, 2323–2334.

Giansanti, M.G., Bonaccorsi, S., Williams, B., Williams, E.V., Santolamazza, C., Goldberg, M.L., and Gatti, M. (1998). Cooperative interactions between the central spindle and the contractile ring during *Drosophila* cytokinesis. Genes Dev. *12*, 396–410.

Giansanti, M.G., Gatti, M., and Bonaccorsi, S. (2001b). The role of centrosomes and astral microtubules during asymmetric division of *Drosophila* neuroblasts. Development *128*, 1137–1145.

Glotzer, M. (2001). Animal cell cytokinesis. Annu. Rev. Cell Dev. Biol. *17*, 351–386.

Gunsalus, K., Bonaccorsi, S., Williams, E., Vernì, F., Gatti, M., and Goldberg, M.L. (1995). Mutations in *twinstar*, a *Drosophila* gene encoding a Cofilin/ADF homologue, result in defects in centrosome migration and cytokinesis J. Cell Biol. *131*, 1–17.

Herrmann, S., Amorim, I., and Sunkel, C.E. (1998). The POLO kinase is required at multiple stages during spermatogenesis in *Drosophila melanogaster*. Chromosoma *107*, 440–451.

Hime, G.R., Brill, J.A., and Fuller, M.T. (1996). Assembly of ring canals in the male germ line from structural components of the contractile ring. J. Cell Sci., *109*, 2779–2788.

Hime, G., and Saint, R. (1992). Zygotic expression of the *pebble* locus is required for cytokinesis during the postblastoderm mitoses of *Drosophila*. Development *114*, 165–171.

Jantsch-Plunger, V., and Glotzer, M. (1999). Depletion of syntaxins in the early *Caenorhabditis elegans* embryo reveals a role for membrane fusion events in cytokinesis. Curr. Biol. *9*, 738–745.

Jantsch-Plunger, V., Gonczy, P., Romano, A., Schnabel, H., Hamill, D., Schnabel, R., Hyman, A.A., and Glotzer, M. (2000). CYK-4: a Rho family GTPase activating protein (GAP) required for central spindle formation and cytokinesis. J. Cell Biol. *149*, 1391–1404.

Karess, R.E., Edwards, K.A., Kulkarni, S., Aguilera, I., and Kiehart, D.P. (1991). The regulatory light chain of nonmuscle myosin is encoded by *spaghetti-squash*, a gene required for cytokinesis in *Drosophila*. Cell *65*, 1177–1189.

Lauber, M.H., Waizenegger, I., Steinmann, T., Schwarz, H., Mayer, U., Hwang, I., Lukowitz, W., and Jurgens, G. (1997). The *Arabidopsis* KNOLLE protein is a cytokinesis-specific syntaxin. J. Cell Biol. *139*, 1485–1493.

Lehner, C.F. (1992). The *pebble* gene is required for cytokinesis in *Drosophila*. J. Cell Sci. *103*, 1021–1030.

Lindsley, D.L., and Zimm, G.G. (1992). The Genome of *Drosophila melanogaster*, San Diego: Academic Press.

Mastronarde, D.N., McDonald, K.L., Dijng, R., and McIntosh, J.R. (1993). Interpolar spindle microtubules in PtK cells. J. Cell Biol. *123*, 1474–1489.

Mishima, M., Kaitna, S., and Glotzer, M. (2002). Central spindle assembly and cytokinesis require a kinesin-like protein/RhoGAP complex with microtubule bundling activity. Dev. Cell *2*, 41–54.

Palazzo, A.F., Cook, T.A., Alberts, A.S., and Gundersen, G.G. (2001). mDia mediates Rho-regulated formation and orientation of stable microtubules. Nat. Cell Biol. *8*, 723–729.

Powers, J., Bossinger, O., Rose, D., Strome, S., and Saxton, W. (1998). A nematode kinesin required for cleavage furrow advancement. Curr. Biol. *8*, 1133–1136.

Prokopenko, S.N., Brumby, A., O'Keefe, L., Prior, L., He, Y., Saint, R., and Bellen, H.J. (1999). A putative exchange factor for Rho1 GTPase is required for initiation of cytokinesis in *Drosophila*. Genes Dev. *13*, 2301–2314.

Prokopenko, S.N., Saint, R., and Bellen, H.J. (2000). Untying the Gordian knot of cytokinesis. Role of small G proteins and their regulators. J. Cell Biol. *148*, 843–848.

Raich, W.B., Moran, A.N., Rothman, J.H., and Hardin, J. (1998). Cytokinesis and midzone microtubule organization in *Caenorhabditis elegans* require the kinesin-like protein ZEN-4. Mol. Biol. Cell *9*, 2037–2049.

Regan, C.L., and Fuller, M.T. (1990). Interacting genes that affect microtubule function in *Drosophila melanogaster*: two classes of mutations revert the failure to complement between *haync2* and mutations in tubulin genes. Genetics *125*, 77–90.

Shuster, C.B., and Burgess, D.R. (2002). Targeted new membrane addition in the cleavage furrow is a late, separate event in cytokinesis. Proc. Natl. Acad. Sci. USA *99*, 3633–3638.

Skop, A.R., Bergmann, D., Mohler, W.A., and White, J.G. (2001). Completion of cytokinesis in *C. elegans* requires a brefeldin A-sensitive membrane accumulation at the cleavage furrow apex. Curr. Biol. *11*, 735–746.

Somers, W.G., and Saint, R. (2003). A RhoGEF and Rho Family GTPase-Activating protein complex links the contractile ring to cortical microtubules at the onset of cytokinesis. Dev. Cell *4*, 29–39.

Somma, M.P., Fasulo, B., Cenci, G., Cundari, E., and Gatti, M. (2002). Molecular dissection of cytokinesis by RNA interference in *Drosophila* cultured cells. Mol. Biol. Cell *13*, 2448–2460.

Sunkel, C.E., and Glover, D.M. (1988). polo, a mitotic mutant of *Drosophila* displaying abnormal spindle poles. J. Cell Sci. *89*, 25–38.

Straight, A.F., and Field, C.M. (2000). Microtubules, membranes and cytokinesis. Curr. Biol. *10*, 760–770.

Ungar, D., Oka, T., Brittle, E.E., Vasile, E., Lupashin, V.V., Chatterton, J.E., Heuser, J.E., Krieger, M., and Waters, M.G. (2002). Characterization of a mammalian Golgi-localized protein complex, COG, that is required for normal Golgi morphology and function. J. Cell Biol. *157*, 405–415.

Xu, H., Brill, J.A., Hsien, J., Boulianne, G.L., and Trimble, W.S. (2002). Syntaxin 5 is required for cytokinesis and spermatid differentiation in *Drosophila*. Dev. Biol. *251*, 294–306.

Wassermann, S. (1998). FH proteins as cytoskeletal organizers. Trends Cell Biol. *8*, 111–115.

Williams, B.W., Riedy, M.F., Williams, E.V., Gatti, M., and Goldberg, M.L. (1995). The *Drosophila* Kinesin-like protein KLP3A is a midbody component required for central spindle assembly and initiation of cytokinesis. J. Cell Biol. *129*, 709–723.